Cerebral Cortex, December 2016;26: 4435–4449

doi: 10.1093/cercor/bhw315
Advance Access Publication Date: 12 October 2016
Original Article

ORIGINAL ARTICLE

Extending the Cortical Grasping Network: Pre-supplementary Motor Neuron Activity During Vision and Grasping of Objects

Marco Lanzilotto[1,†], Alessandro Livi[1,†], Monica Maranesi[2], Marzio Gerbella[1,2], Falk Barz[3,4], Patrick Ruther[3,4], Leonardo Fogassi[1], Giacomo Rizzolatti[2], and Luca Bonini[1,2]

[1]Department of Neuroscience, University of Parma, 43125 Parma, Italy, [2]Istituto Italiano di Tecnologia (IIT), Brain Center for Social and Motor Cognition (BCSMC), 43125 Parma, Italy, [3]Department of Microsystems Engineering (IMTEK), University of Freiburg, 79110 Freiburg, Germany, and [4]BrainLinks-BrainTools Cluster of Excellence, University of Freiburg, 79110 Freiburg, Germany

Address correspondence to Marco Lanzilotto and Luca Bonini, Department of Neuroscience, University of Parma, via Volturno 39, 43125 Parma, Italy. E-mail: marco.lanzilotto@unipr.it; luca.bonini@unipr.it

[†]These authors contributed equally to this work.

Abstract

Grasping relies on a network of parieto-frontal areas lying on the dorsolateral and dorsomedial parts of the hemispheres. However, the initiation and sequencing of voluntary actions also requires the contribution of mesial premotor regions, particularly the pre-supplementary motor area F6. We recorded 233 F6 neurons from 2 monkeys with chronic linear multishank neural probes during reaching–grasping visuomotor tasks. We showed that F6 neurons play a role in the control of forelimb movements and some of them (26%) exhibit visual and/or motor specificity for the target object. Interestingly, area F6 neurons form 2 functionally distinct populations, showing either visually-triggered or movement-related bursts of activity, in contrast to the sustained visual-to-motor activity displayed by ventral premotor area F5 neurons recorded in the same animals and with the same task during previous studies. These findings suggest that F6 plays a role in object grasping and extend existing models of the cortical grasping network.

Key words: macaque, multielectrode probes, reaching–grasping, visuomotor neurons

Introduction

According to the most widely accepted view, the cortical organization of visually guided grasping actions in primates depends mainly on the primary motor cortex and a network of reciprocally interconnected parietal and premotor areas lying on the dorsolateral and dorsomedial portions of the cerebral hemispheres (Rizzolatti and Luppino 2001; Grafton 2010; Davare et al. 2011; Fattori et al. 2015; Kaas and Stepniewska 2016).

Neurophysiological studies in the monkey have revealed that the anterior intraparietal area (AIP; Sakata et al. 1995; Baumann et al. 2009), the posterior parietal area V6A (Fattori et al. 2010; Fattori et al. 2012), the ventral premotor area F5

(Murata et al. 1997; Raos et al. 2006; Fluet et al. 2010; Bonini et al. 2014a; Vargas-Irwin et al. 2015), and the ventro-rostral portion of the dorsal premotor area F2 (Raos et al. 2004; Vargas-Irwin et al. 2015) host visuomotor neurons that discharge during both the visual presentation of target objects and the execution of reaching–grasping actions. These areas form a rich set of parieto-frontal circuits that underlie the visuomotor transformations of object properties into the most appropriate motor acts to interact with it (see Maranesi et al. 2014). However, motor representations encoded in this grasping network need to be selected, triggered, or inhibited in order to appropriately turn them into action. This latter function is typically associated with the pre-supplementary motor cortex, defined as area F6 in macaques (Matelli et al. 1991).

Area F6 constitutes a bridge between prefrontal regions and the dorsolateral premotor areas (F2, F4, and F5) related to the organization and control of forelimb actions (Rizzolatti and Luppino 2001). Intracortical microstimulation (ICMS) studies in monkeys have demonstrated that area F6 controls complex multijoint forelimb movements (Luppino et al. 1991). Furthermore, pioneering neurophysiological studies with ethological techniques (Rizzolatti et al. 1990) have shown that area F6 neurons discharged during reaching–grasping movements, but "did not appear to be influenced by how the objects were grasped nor by where they were located." These findings suggested that F6 "plays a role in the preparation of reaching–grasping arm movements and in their release when the appropriate conditions are set" (Rizzolatti et al. 1990) but it is not involved in the encoding of specific motor aspects, such as object/grip features. Along the same lines, subsequent neurophysiological studies on area F6 focused on fairly simple limb movements whose temporal/sequential organization, initiation, and stopping were instructed by sensory cues, but they did not investigate manipulative actions (Tanji 2001; Nachev et al. 2008), thus leaving unknown whether and to what extent F6 is involved also in visuomotor processing of objects for grasping.

The present study is the first to provide evidence that F6 neurons contribute to the encoding of target objects and grip types. Furthermore, by recording area F6 neurons from the same animals and with the same tasks previously employed to characterize the activity of the hand sector of area F5 (Bonini et al. 2014a; Maranesi et al. 2015), we were able to compare the functional properties of the 2 regions. Based on these findings, we conclude that area F6 should be considered an additional node of the widely accepted brain network for object grasping.

Materials and Methods

Experiments were carried out on one Macaca nemestrina (MK1, male, 9 kg) and one Macaca mulatta (MK2, male, 7 kg). Before recordings, monkeys were habituated to sit in a primate chair and to interact with the experimenters. They were then trained to perform the visuomotor tasks described below using the hand contralateral to the hemisphere to be recorded. When the training was completed, a head-fixation system was implanted under general anesthesia (ketamine hydrochloride, 5 mg/kg i.m. and medetomidine hydrochloride, 0.1 mg/kg i.m.), followed by postsurgical pain medications. Surgical procedures were the same as previously described (Bruni et al. 2015). All experimental protocols complied with the European law on the humane care and use of laboratory animals (directives 86/609/EEC, 2003/65/CE, and 2010/63/EU), they were authorized by the Italian Ministry of Health (D.M. 294/2012-C and 11/12/2012), and approved by the Veterinarian Animal Care and Use Committee of the University of Parma (Prot. 78/12 17/07/2012).

Apparatus and Behavioral Paradigm

Both monkeys were trained to perform the visuomotor task described in previous works (see Bonini et al. 2014a; Maranesi et al. 2015). The monkey was seated on a primate chair in front of a box, shown in Figure 1A from the monkey's point of view. The box was divided horizontally into 2 sectors by a half-mirror: the upper sector contained a small black tube with a white light-emitting diode (LED) that could project a spot of light on the half-mirror surface; the lower sector contained a sliding plane hosting three different objects. When the LED was turned on (in complete darkness), the half-mirror reflected the spot of light so that it appeared to the monkey as located in the lower sector (fixation point), in the exact position of the center of mass of the not-yet-visible target object. The objects—a ring, a small cone, and a big cone—were chosen because they afforded three different grip types, as follows: hook grip (in which the index finger enters the ring); side grip (performed by opposing the thumb and the lateral surface of the index finger); whole-hand prehension (achieved by opposing all the fingers to the palm). Objects were presented, one at a time during different experimental trials, through a 7-cm opening located on the monkey's sagittal plane at a reaching distance from its hand starting position. A stripe of white LEDs located on the lower sector of the box allowed us to illuminate it during specific phases of the task. Note that, because of the half-mirror, the fixation point remained visible in the middle of the object even when the lower sector of the box was illuminated.

The task included three basic conditions, as illustrated in Figure 1B: grasping in the light, grasping in the dark, and a no-go condition. Each of them started when the monkey held its hand on a fixed starting position, after a variable intertrial period ranging from 1 to 1.5 s from the end of the previous trial.

1. *Grasping in the light*: the fixation point was presented and the monkey was required to start fixating it within 1.2 s. Fixation onset resulted in the presentation of a cue sound (a pure high tone constituted by a 1200 Hz sine wave), which instructed the monkey to grasp the subsequently presented object (go-cue). After 0.8 s, the lower sector of the box was illuminated and one of the objects became visible. Then, after a variable time lag (0.8–1.2 s), the sound ceased (go-signal), at which point the monkey had to reach, grasp, and pull the object within 1.2 s. It then had to hold the object steadily for at least 0.8 s. If the task was performed correctly without breaking fixation, the reward was automatically delivered (pressure reward delivery system, Crist Instruments).
2. *Grasping in the dark*: the entire temporal sequence of events in this condition was identical to that of grasping in the light. However, when the cue sound (the same high tone as in grasping in the light) ceased (go-signal), the light inside the box was automatically switched off and the monkey performed the subsequent motor acts in complete darkness. Note that because the fixation point was visible for the entire duration of each trial, it provided a spatial guidance for reaching the object in the absence of visual feedback. In this paradigm, grasping in the light and grasping in the dark trials were identical and unpredictable until the occurrence of the go-signal: thus, action planning was the same in both conditions, and the only difference between them was the presence/absence of visual feedback from the acting hand and the target object.
3. *No-go condition*: the basic sequence of events in this condition was the same as in the other go conditions, but a different cue sound (a pure low tone constituted by a 300-Hz sine

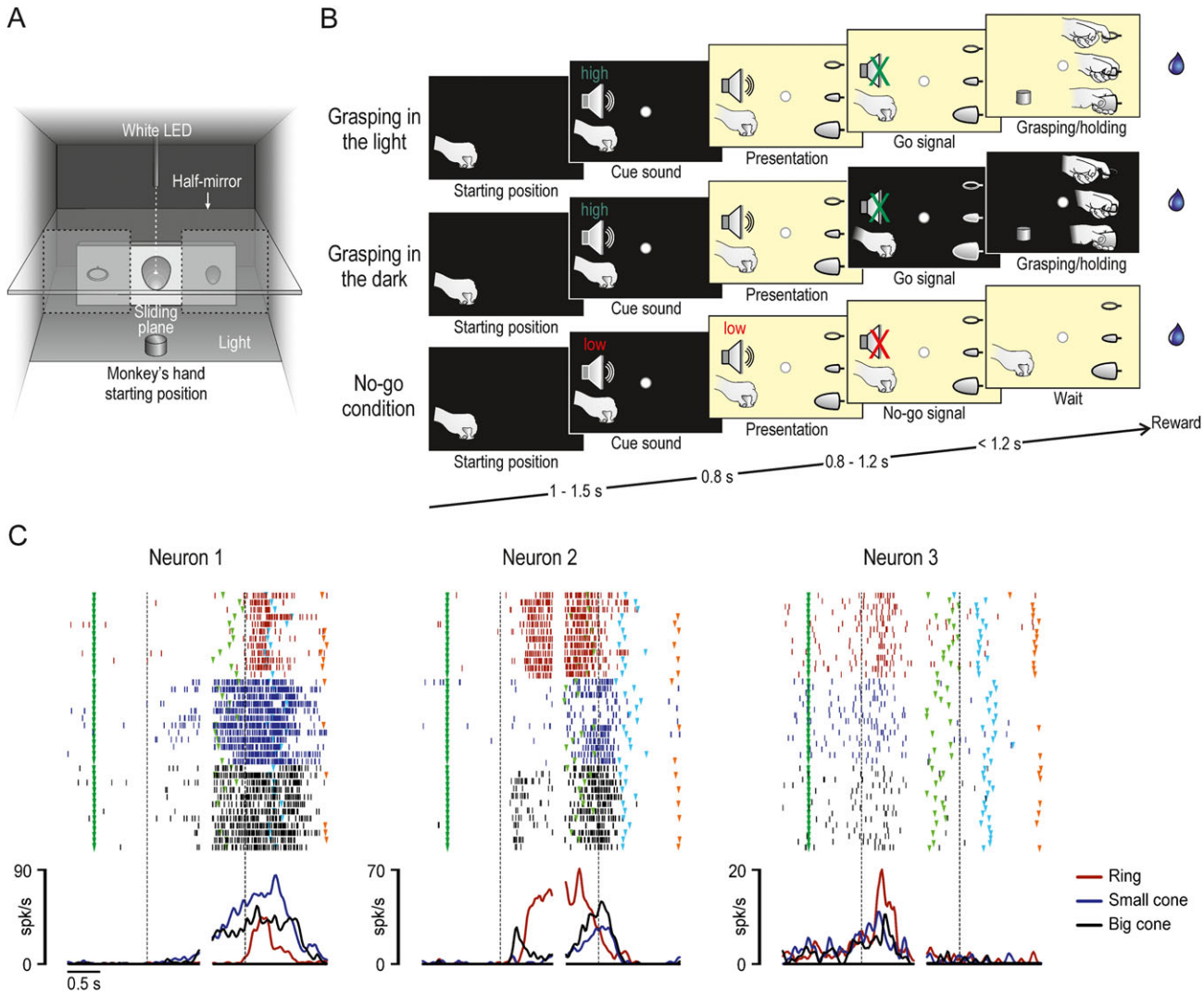

Figure 1. Behavioral task and example neurons. (*A*) Box and task apparatus seen from the monkey's point of view. (*B*) Stages of the three main conditions of the task: grasping in the light, grasping in the dark, and no-go condition. (*C*) Examples of the three main types of neurons recorded during task execution in the light. For each neuron rasters and spike density function are aligned (dashed lines) on object presentation (left part) and, after the gap, on the moment when the monkey's hand detached from the starting position (right part). Markers: dark green, cue sound onset (beginning of the trial); light green, end of the cue sound (go-signal); light blue, object pulling onset; orange, end of the trial and reward delivery.

wave) instructed the monkey to remain still and continue fixating the object for 1.2 s in order to receive a drop of juice as a reward. The same sequence of events of the no-go condition has also been employed during a barrier test. In the barrier test, a transparent plastic barrier was interposed between the monkey's hand and the target. The aim of this test was to verify whether object processing by F6 neurons could be different depending on whether the monkey refrained from acting because of a physical obstacle (the barrier) or because of an instruction cue (the no-go signal). Hence, we used the go-cue during this test in order to ensure that the monkey refrained from acting because of the presence of the barrier (see also Bonini et al. 2014a). Before formal testing of neuronal activity, the monkey was administered a few trials before starting the acquisition block, in order to ensure it actually understood that the barrier was present.

The task phases were automatically controlled and monitored by LabView-based software, enabling the interruption of the trial if the monkey broke fixation, made an incorrect movement, or did not respect the task temporal constraints described above. In all these cases, no reward was delivered. After correct completion of a trial, the monkey was automatically rewarded with the same amount of juice in all conditions.

The activity of each neuron was recorded in at least 12 trials for each basic condition. In all sessions, we also recorded 12 additional control trials in which the monkey was presented, in complete darkness and with its hand still on the starting position, with the fixation point alone: after a variable time lag (<1 s) from fixation onset, the reward was delivered. These trials were used to verify the possible presence of neuronal responses due to mouth movements/reward delivery, which could otherwise be confounded with hand-related activity, particularly during the holding epoch that precedes the reward delivery. Neurons responding specifically to this condition were not considered as task related in the present study.

Recording and Intracortical Microstimulation Techniques

Neuronal recordings were performed by means of chronically implanted 2D or 3D arrays of linear silicon probes with 8 recording channels per shaft and a variable number of shafts per probe, as follows: one 4-shaft 2D probe in the right hemisphere of MK1; one 4-shaft 2D probe, and one 3D probe in the left hemisphere of MK1; two 3D probes in the right hemisphere of MK2 (see Supplementary Fig. S1). All probes were implanted vertically, approximately 1 mm laterally to the mesial wall (see Fig. 2). Previous reports provide more details on the methodology of probe fabrication (Herwik et al. 2011), assembly (Barz et al. 2014), and implantation (Bonini et al. 2014).

The signal was amplified and sampled at 40 kHz with a 16-channel Omniplex recording system (Plexon). Different sets of 16 channels were recorded only one time during separate sessions on different days. Online spike sorting was performed on all channels using dedicated software (Plexon), but all final quantitative analyses were performed off-line, as described in the subsequent sections.

ICMS was performed, in MK2, through all the recording sites at the end of the recording sessions. Monopolar, biphasic trains of cathodic square wave pulses were delivered through a constant current stimulator (PlexStim, Plexon), with the following parameters: total train duration 500 ms, single pulse width 0.2 ms, and pulse frequency 300 Hz. The current intensity ranged from 20 to 100 μA and was controlled on an oscilloscope by measuring the voltage drop across a 10-kΩ resistor in series with the stimulating electrode. At each site, ICMS was delivered when the monkey was quiet and relaxed, and those cases in which monkeys performed voluntary movements were not used to establish the stimulation threshold. Movements were considered to be evoked by ICMS when 2 experimenters, observing the animal during pulse delivery, independently and repeatedly identified the same joint displacement or muscular twitch, according to previous ICMS studies of the same area (Luppino et al. 1991). The threshold was defined as the lowest current intensity capable of evoking movements in 50% plus one of the stimulations delivered (usually 4 out of 6, or 5 out of 8 stimulations).

Recording of Behavioral Events and Definition of Epochs of Interest

Distinct contact sensitive devices (Crist Instruments) were used to detect when the monkey (grounded) touched with the hand the metal surface of the starting position or one of the target objects. To signal the onset and tonic phase of object pulling, an additional device was connected to the switch located behind each object. Each of these devices provided a TTL signal, which was used by the LabView-based software to monitor the monkey's performance and to control the generation and presentation of the behavioral paradigm's auditory and visual cue signals.

Eye position was monitored in parallel with neuronal activity with an eye tracking system consisting of a 50-Hz CCD video camera provided with an infrared filter and 2 spots of infrared light. Analog signal related to horizontal and vertical eye positions was fed to a computer equipped with dedicated software, enabling calibration and basic processing of eye position signals. The monkey was required to maintain its gaze on the fixation point (tolerance radius 5°) throughout the task, and the eye position signal was monitored by the same LabView-based software dedicated to the control of the behavioral paradigm.

The same software also generated different digital output signals associated with auditory and visual stimuli, the target object presented in each trial, the reward delivery and possible errors made by the monkey during the task (i.e., when the monkey broke fixation). These signals, together with the TTL signals related to the main behavioral events described above, were fed to the Omniplex system to be recorded together with the neuronal activity and subsequently used to construct the response histograms and the data files for statistical analysis.

Single-neuron activity was analyzed in relation to the digital signals related to the main behavioral events, by considering the following epochs of interest: 1) baseline, 500 ms before object presentation; 2) object presentation, from 0 to 500 ms after switching on the light; 3) premovement, 500 ms before reaching onset, signaled by the detachment of monkey's hand from the starting position (since an actual movement of the arm does occur to detach the hand from the starting position, this epoch has been considered among those used for the study of motor-related activity); 4) reaching–grasping, from reaching onset to pulling onset (of variable duration, calculated on a trial-by-trial basis); 5) object holding, from pulling onset to 500 ms after this event. Note that during baseline, the monkey rested its hand unmovingly on the starting position, was staring at the fixation point, and was already aware of whether the ongoing trial was a go or a no-go trial: these features enabled us to assess possible variation in neural discharge specifically linked with the subsequent task stages within the ongoing behavioral set.

Off-line analysis of electromyographic activity of proximal and distal forelimb muscles during task execution has been previously described in both monkeys employed for the present study (Bonini et al. 2014b), and allowed us to exclude the possible presence of preparatory motor activity during no-go trials and baseline epoch.

Data Analyses

The raw signals were high-pass filtered off-line (300 Hz). Single units were then isolated using principal component and template matching techniques provided by dedicate off-line sorting software (Plexon) (Bonini et al. 2014). After identification of well-isolated single units, we classified neurons significantly activated during movement-related epochs relative to baseline, both during grasping in the light and grasping in the dark, separately. For this purpose, we employed a 3×4 repeated measures ANOVA (factors: Object and Epoch). We classified as "motor" all neurons showing, at least during the grasping-in-the-dark condition, a significant main effect of the factor Epoch and/or an interaction between the 2 factors ($P < 0.05$), and whose discharge differed from baseline during at least one of the three movement-related epochs (premovement, reaching–grasping, and pulling) relative to baseline for at least one of the three target objects (Bonferroni post hoc tests, $P < 0.05$).

Possible responses to object presentation relative to baseline were assessed considering both conditions (go and no-go) by means of a $2 \times 3 \times 2$ repeated measures ANOVA (factors: Condition, Object, and Epoch), with a significance criterion of $P < 0.05$. Only neurons showing at least a significant effect of the factor Epoch, alone or in interaction with one or both of the other factors, were classified as visually-triggered (Bonferroni post hoc tests, $P < 0.05$). Single-neuron response to the visual presentation of the objects during the barrier test were

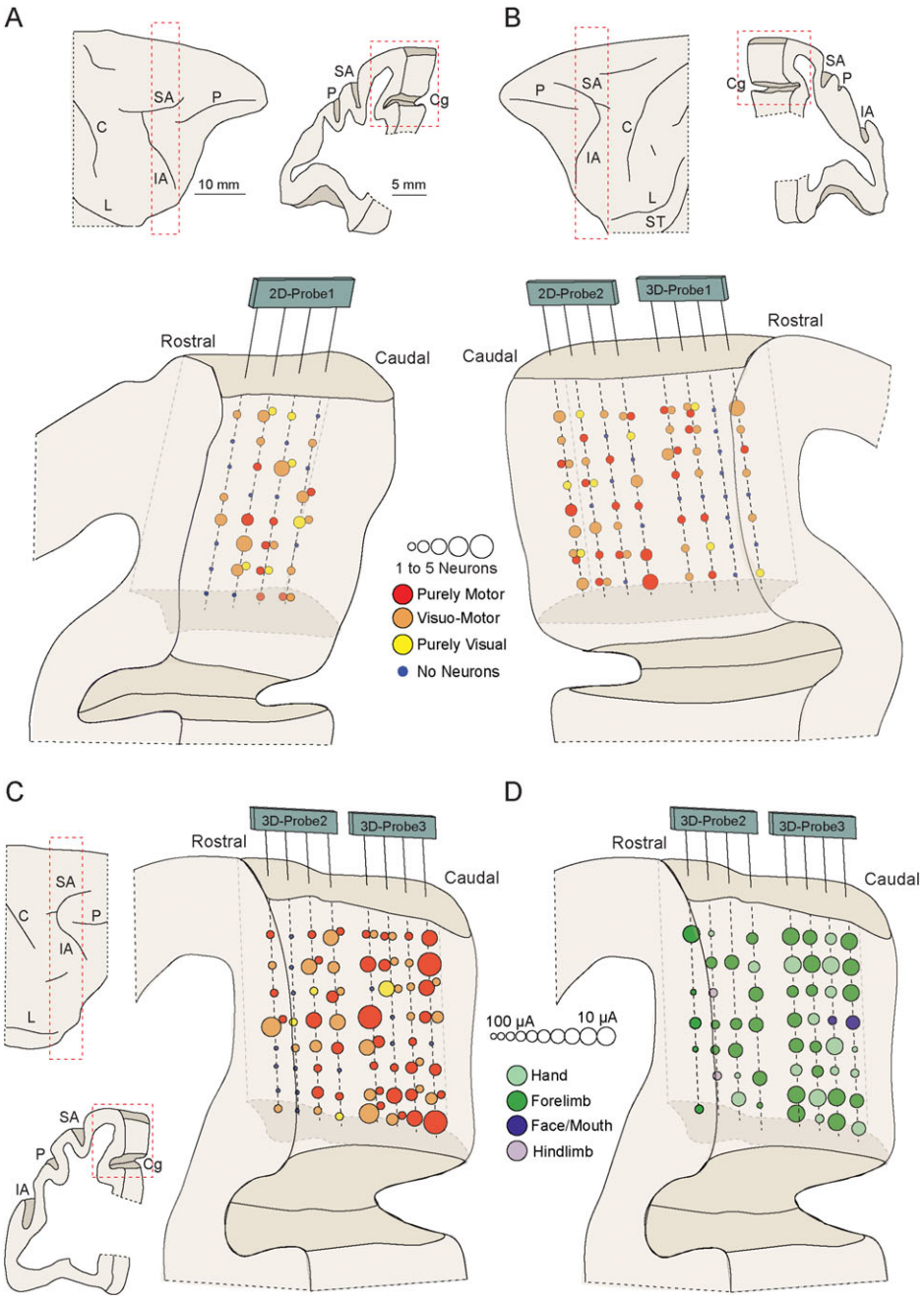

Figure 2. Reconstruction of the recorded regions and functional maps. Anatomical reconstruction of the right (*A*) and left (*B*) hemispheres of MK1, with superimposed number and class of neurons recorded from each site. In (*B*), each "site" of the (rostral) 3D probe (see Materials and Methods) includes neurons recorded from pairs of adjacent electrodes (not shown) spaced by 300 µm (see also Supplementary Fig. S1). (*C*) Anatomical reconstruction of the right hemisphere of MK2, with superimposed number and class of neurons recorded from each site of the 3D probes. Conventions as in panel (*B*). (*D*) Results of an ICMS mapping study carried out on MK2 at the end of the recordings. Note that 2 sites on the most caudal part of the recorded region were associated with face–mouth movement, which is known to correspond to the functional border between areas F3 (caudally) and F6 (rostrally) (see Luppino et al. 1991). The size of the circles corresponds to the current intensity threshold (see Materials and Methods). Scale bars in (*A*) also applies to (*B*) and (*C*). C, central sulcus; Cg, cingulate sulcus; IA, inferior arcuate sulcus; L, Lateral sulcus; SA, superior arcuate sulcus; ST, superior temporal sulcus.

analyzed by means of a 3×2 repeated measures ANOVA (factors: Object and Epoch), with a criterion of $P < 0.05$.

Population analyses were carried out taking into account single-neuron responses expressed in terms of normalized mean activity, as previously described elsewhere (see Bonini et al. 2010), and analyzed with different repeated measures ANOVAs depending on the conditions to be compared (as described in the figure captions).

For each of the recorded neurons, we also calculated the timing of the motor-activity peak. For this purpose, we considered the averaged activity across 12 trials of the same condition in bins of 100 ms, slit forward in steps of 20 ms, within a time window ranging from 500 ms before movement onset to 1 s after this event: the timing associated with the highest among all the obtained values was considered the peak of activity timing. Furthermore, relative to each neuron peak of activity (equal

to 1), we also calculated the burst duration as the time interval between the first bin before and after the peak of activity whose value was higher and lower than $(1-B)\times 0.25 + B$, respectively, where B is the mean baseline activity.

Finally, one-way repeated measures sliding ANOVAs (factor: Object, three levels) were used to verify, for each neuron, possible differences ($P < 0.05$ uncorrected) in terms of the firing rate associated with the different objects over time. This analysis was performed in 500 ms epochs, slit forward in steps of 20 ms, from 500 ms before to 1050 ms after object presentation, and from 750 ms before to 1000 ms after movement onset. The results of this analysis were plotted (relative to the center of each epoch) by calculating the percentage of significantly tuned neurons in each epoch within each neuronal population (see Fig. 7).

Anatomical Localization of the Recorded Region

The histological analysis aimed at identifying the exact location of the implanted probes was performed in both hemispheres of MK1. For this purpose, at the end of the experiment, MK1 was anaesthetized with ketamine hydrochloride (15 mg/kg i.m.) followed by an intravenous lethal injection of pentobarbital sodium and perfused with saline, 4% paraformaldehyde, and 5% glycerol, prepared in 0.1M phosphate buffer, pH 7.4, through the left cardiac ventricle. The brain was subsequently removed from the skull, photographed and then frozen and cut into coronal sections of 60-μm thickness. The locations of the electrode tracks in the cortex were assessed under an optical microscope in Nissl-stained sections and then plotted and digitized together with the outer and inner borders of the cerebral cortex using a computer-based charting system (for the details of the procedure, see Gerbella et al. 2016). The cytoarchitectonic features of the recorded region were identified based on the criteria used to subdivide the mesial frontal areas by Matelli et al. (1991) (Belmalih et al. 2007). To obtain monkey 3D volumetric brain reconstructions, containing the data regarding the location of the probes' traces, the data from individual sections were also imported into homemade software (Bettio et al. 2001), allowing us also to cut the brain in slices of different planes and thickness. Finally, the schematic drawing of the implanted probes was superimposed on the exact location of their traces on oblique re-sliced views of the 3D reconstructions in both hemispheres.

In MK2, which had not yet been sacrificed, the location of the recorded sites was reconstructed based on MRI scan of the monkey's brain performed before the implantation of the head-fixation system and the probes. To obtain a visualization comparable to the one of MK1, MRI slices were directly imported into the aforementioned 3D reconstruction software, together with the stereotaxically measured location of the implanted arrays, in order to obtain the 3D reconstruction as described above.

Results

We recorded a total of 355 single neurons with the task illustrated in Figure 1B (see Bonini et al. 2014a; Maranesi et al. 2015, see Materials and Methods for more details), of which 233 (65.6%) were classified as task related based on the statistical analysis of their response during the different conditions and epochs of the task (see Materials and Methods).

General Properties of Area F6 Neurons Recorded During the Visuomotor Task

Among the task-related neurons, 108 were purely motor, 103 were visuomotor, and 22 were purely visual neurons. Example neurons are shown in Figure 1C. Neurons classified as purely motor discharged only during reaching–grasping execution (Neuron 1). Visuomotor neurons became active during both the object presentation epoch and reaching–grasping execution (Neuron 2): as exemplified by this neuron, the motor-related discharge of visuomotor neurons was typically characterized by early onset and extremely different dynamics depending on the tested object, often with clearly distinct peaks of visual and motor activity. Finally, purely visual neurons discharged only during object presentation (Neuron 3). Note that all these example neurons also showed differential activation depending on the target object. Extensive details on all the recorded neurons' motor and visual preferences for the target object are provided in Table 1, as well as in the following sections.

Anatomical and Functional Characterization of the Recorded Regions

Neurons were recorded from five chronic arrays constituted by different configurations of linear multielectrode silicon probes (see Supplementary Fig. S1), all implanted in area F6. Figure 2 shows the exact location of the recorded regions in both animals by superimposing a schematic drawing of the implanted probes on 3D reconstructions of the monkey's brain. The recorded regions in both hemispheres of MK1 (Fig. 2A and B) have been reconstructed based on the histological identification of the probes' tracks from Nissl-stained coronal sections of the monkey's brain (see Materials and Methods and Supplementary Fig. S2). The architectonic features of both recorded regions in MK1 indicate that all probes were located within the anatomical borders of area F6 (Supplementary Fig. S2). Because MK2 had not yet been sacrificed, the reconstruction of the recording sites of the 2 probes implanted in its right hemisphere (Fig. 2C) was performed with the same software and methodology (see Materials and Methods) but based on magnetic resonance imaging (MRI) slices of the monkey's brain. Figure 2 also shows that visually-triggered neurons (i.e., visual and visuomotor) and purely motor neurons were largely intermingled in both animals and were recorded even from the

Table 1 Object preference of all the recorded neurons

Neuron class	Ring	Small cone	Big cone	Two objects	Unselective	Total
Purely motor[a]	11	6	7	8	76	108
Visuomotor[a]	13	2	2	5	81	103
Purely visual[a]	5	0	0	1	16	22
Total	29	8	9	14	173	233

Note: [a]For purely motor neurons, object preference was considered during reaching–grasping execution epochs, whereas for visuomotor and purely visual neurons, object preference was considered during the target presentation epoch.

same contact in about 30% of the sites in which single unit activity was detected.

Figure 2D also shows the results of long-train ICMS carried out in MK2 (500-ms biphasic cathodic pulses at 300 Hz). In particular, we observed complex, multijoint, and relatively slow movements involving the contralateral arm and the shoulder, often including the wrist and the hand (dark green circles in Fig. 2D) and, in some cases, even synergic finger movements alone (light green circles). These findings are in line with previous ICMS studies on area F6 (Luppino et al. 1991), and indicate that neuronal activation in this region plays a role in the control of proximal as well as distal movements of the contralateral forelimb.

Purely Motor Neurons

Most purely motor neurons (n = 75, 69.4%) discharged similarly during reaching–grasping in the light and in the dark, although some showed a stronger discharge either in the light (n = 23, 21.30%) or in the dark (n = 10, 9.3%). Among purely motor neurons, 32 (29.6%) discharged differently depending on the grasped object. Figure 3A shows examples of grip-selective F6 motor neurons tested during reaching–grasping in the light and in the dark. Neuron 1 is a typical example of a grip-selective neuron, which discharged more strongly when the monkey grasped the ring regardless of whether grasping was performed in the light or in the dark. Neuron 2 exhibited a preferential discharge for the big cone, but its activity was stronger during grasping in the light, whereas Neuron 3 showed the opposite modulation, being more strongly activated during grasping in the dark than in the light, with a preferential discharge for the big and small cones relative to the ring. It is clear from the neuron examples that the target selectivity of F6 purely motor neurons cannot be accounted for by vision of the object. This conclusion is also supported by population activity, which shows that both motor activity and object selectivity assessed during grasping in the light remained the same even during grasping in the dark (Fig. 3B).

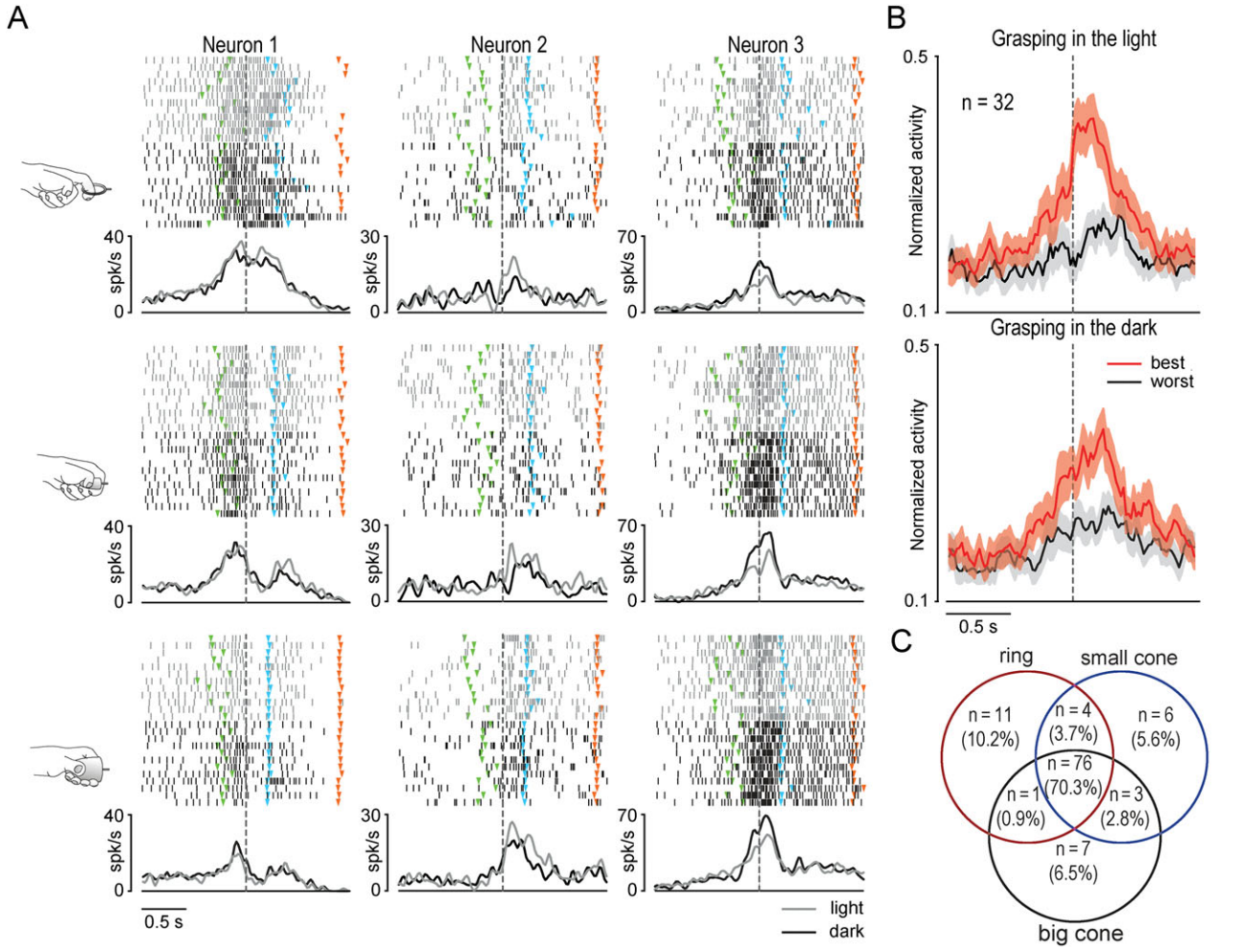

Figure 3. Functional properties of F6 purely motor neurons. (*A*) Examples of three F6 purely motor neurons showing selectivity for the target object. The image on the left of each line of the panel shows the type of grip employed by the monkey in that trials. Other conventions and markers as in Figure 1. (*B*) Population activity of purely motor neurons with object selectivity. As for single-neuron examples, the activity is aligned to the movement onset, and shows the averaged population response to the preferred and non-preferred target established on the basis of each neurons response during grasping in the light. The colored shaded area around each curve represents 1 standard error. By means of 2 × 3 repeated measures ANOVAs (factors: Object and Epoch) applied to each condition (light and dark), separately, we observed that this neuronal population responded and showed object selectivity during both premovement and reaching–grasping in the dark ($P < 0.001$) as well as in the light ($P < 0.001$). Furthermore, the population response to each object (best and worst) in the light was not significantly different from that to the same object grasped in the dark, neither during the premovement (best $t = 0.076$, $P = 0.94$; worst $t = 0.40$, $P = 0.69$) nor in the reaching–grasping (best $t = 2.01$, $P = 0.052$; worst $t = 0.61$, $P = 0.55$) epoch. (*C*) Number of purely motor neurons with selectivity for 1 or 2 of the target objects, or with no object selectivity.

Interestingly, neuronal preference for the three tested objects was substantially balanced: indeed, we did not observe any prevalence either in terms of the number of single neurons that showed a preference for a particular object (χ^2 = 1.75, P = 0.42, Fig. 3C) or in terms of the overall intensity of population activity during the grasping of each of the objects (Supplementary Fig. S3). Altogether, these findings indicate that the object selectivity of purely motor neurons reliably reflects a motor preference for the type of grip.

Visually-Triggered Neurons

Among the 125 visually-triggered neurons (including both visual and visuomotor neurons), 28 (22.4%) showed object selectivity. Examples are provided in Figure 4A. Neuron 1 is a purely visual neuron that discharged selectively to the presentation of the ring during go trials but not during no-go trials. Note that in spite of its purely visual nature, the response of this neuron was highly context selective, because it encoded the ring only when it was the target of a forthcoming action. A similar selectivity was exhibited by Neuron 2, a visuomotor neuron with a clear-cut preference for the ring during go trials that stopped its firing after the onset of reaching. It is important to note that the discharge of both of these neurons was more closely related to the object presentation than to the reaching–grasping epochs of the task. Although a few F6 visuomotor neurons (e.g., Neuron 3 in Fig. 4A) exhibited a biphasic visual and motor response pattern, this latter activation profile

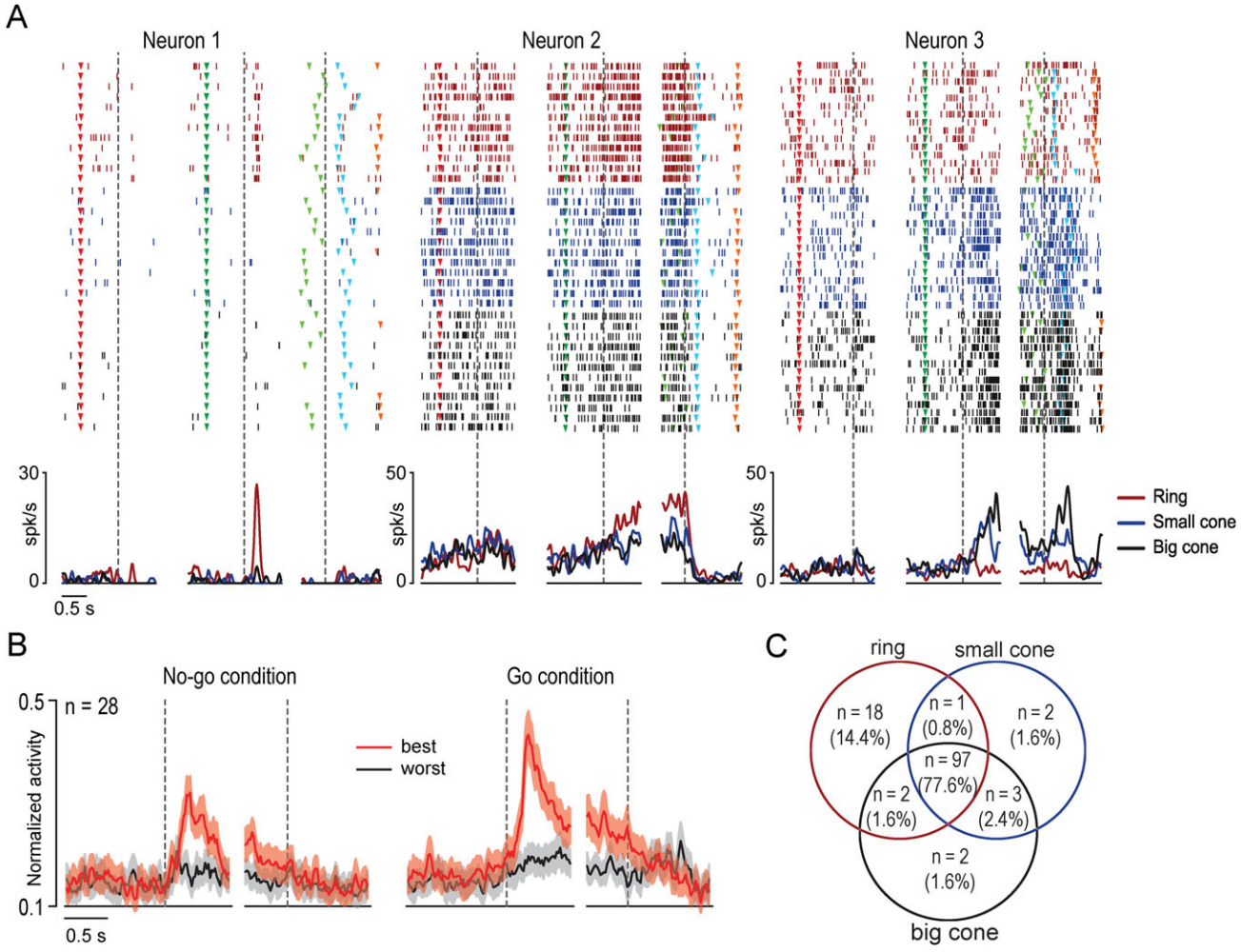

Figure 4. Functional properties of F6 visually-triggered neurons. (*A*) Examples of three F6 visually-triggered neurons showing visual selectivity for the target object. For each neuron, rasters and spike density function have been aligned (dashed lines) to three different events, separated by a gap: 1) object presentation during no-go trials (on the left); 2) object presentation during go trials (on the center); 3) movement onset (on the right). Red triangular marker, no-go cue sound onset (beginning of the trial). Other conventions as in Figure 1. (*B*) Population activity of visually-triggered neurons with object selectivity. Best (red) and worst (gray) objects have been selected, for each neuron, based on the visual response during go-trials. In the no-go condition, the activity is aligned to the object presentation (dashed line on the left) and, after the gap, to the no-go signal (dashed line on the right). In the go condition, the activity is aligned to the object presentation (dashed line on the left) and, after the gap, to the movement onset (dashed line on the right). The population responses to object presentation during the go and no-go conditions have been analyzed separately by means of a 2 × 2 repeated measures ANOVA (factors: Object and Epoch). In both conditions, there was a stronger visual presentation response for the best relative to the worst object ($P < 0.001$), and the population response to this latter did not even reach significance during the no-go condition ($P = 0.18$). Furthermore, the population response to the presentation of the best object was stronger when it occurred during go relative to no-go trials ($t = 4.77$, $P < 0.001$). Another 2 × 3 repeated measures ANOVA (factors: Object and Epoch) has been performed on the movement-related population activity, as well as on the population response aligned to the no-go signal. Interestingly, we found a significant response only for the best object relative to baseline during the premovement epoch ($P < 0.001$) as well as during the epoch preceding the no-go signal ($P < 0.001$), but not during the reaching–grasping epoch. Furthermore, the population activity preceding movement onset and the no-go signal did not differ significantly from each other ($t = 1.85$, $P = 0.075$). (*C*) Number of visually-triggered neurons with visual selectivity for 1 or 2 of the target objects, or with no object selectivity.

was rare, and more importantly, it did not emerge from the population activity profile (Fig. 4*B*). This phenomenon did not depend on the inclusion of purely visual neurons (6 out of 28), because it was present even when only visuomotor neurons were considered (see Supplementary Fig. S4). These findings demonstrate that area F6 neurons can play a role in the visuomotor processing of objects, but their activation dynamic seems to be strikingly different from that of visuomotor neurons described in other brain regions (for a review, see Maranesi et al. 2014, particularly area F5 (Murata et al. 1997; Raos et al. 2006; Bonini et al. 2014a); for a direct comparison, see the following section).

Another important finding is that object visual selectivity displayed by F6 neuronal population during go trials was also present during no-go trials, even though the discharge intensity was significantly reduced. This suggests that visually-triggered F6 neurons underlie visuomotor associations between observed objects and the potential motor actions that can be performed on them. An interesting observation supporting this hypothesis is that visually-triggered neurons exhibited a preferential selectivity for the ring, in contrast to the balanced motor selectivity for the different objects of purely motor neurons (see above), which rules out possible interpretations of this findings in terms of a sampling bias. Indeed, the overrepresentation of the ring was evident both in terms of percentage of single neurons ($\chi^2 = 23.28$, $P < 0.001$, Fig. 4*C*) and in terms of intensity of the overall population response during visual presentation of the ring relative to the other objects (Supplementary Fig. S5). This finding may be due to the well-established role of F6 in forming new arbitrarily learned visuomotor associations (Nakamura et al. 1998). Indeed, whereas the small and big cones were spontaneously grasped with a precision and power grip, respectively, monkeys would naturally grasp a small ring like the one used in this study by means of a side grip with 90° wrist rotation (personal observations) rather than by inserting just the index finger in it (hook grip). This latter grip type was achieved through a specific training, which may explain its visual overrepresentation.

In order to better understand the functional relevance of F6 neurons in object visual processing, we also employed a test previously used to characterize the activity of F5 visuomotor neurons (Bonini et al. 2014a). In this test, carried out on the neurons recorded from MK2 and from the left hemisphere of MK1, a transparent plastic barrier was interposed between the monkey's hand and the target during trials cued with the high tone (go-cue). Note that the monkey was not instructed to refrain from acting (as during no-go trials), but the barrier actually prevented it from reaching and grasping the presented object. An example neuron tested in this condition is shown in Figure 5A. It is evident that this neuron, which discharged more strongly during go trials relative to no-go trials, did also respond during the barrier test, but with a response pattern more closely resembling the one displayed during no-go rather than go trials, even if the auditory cue was the high tone (go-cue). A similar effect was evidenced by the population activity: indeed, the population response was stronger and showed the maximal selectivity during go trials relative to no-go trials, in line with single-neuron behavior, whereas during the barrier test, the discharge intensity was similar to that during no-go trials but completely lacked object selectivity (see Fig. 5*B*). Altogether, these findings indicate that object-selective visual responses of F6 neurons are strongly modulated by the contextual setting: indeed, their selectivity depends mostly on the monkey's intention and possibility to act on the object.

Neuronal Properties and Dynamics in Mesial (F6) and Ventral (F5) Premotor Cortex

According to a widely accepted view, the mesial premotor cortex encodes triggering signals for starting and sequencing self-initiated actions, whose details, such as reach direction and grip type, are processed by dorsolateral premotor areas by means of parieto-premotor interactions (Rizzolatti and Luppino 2001; Cisek and Kalaska 2010; Kaas and Stepniewska 2016). In order to investigate the relative contribution of mesial and ventral premotor areas in reaching–grasping actions, we compared the response properties of neurons recorded from area F6 in this study with those previously recorded from area F5 with the same behavioral paradigm and in the same animals (see Bonini et al. 2014a; Maranesi et al. 2015).

Figure 6*A*–*D* shows the response dynamic of all area F6 recorded neurons with an excitatory response pattern (see also Supplementary Fig. S6 for similar plots of the subset of neurons with inhibitory response) and classified as visuomotor (Fig. 6*A* and *B*) or purely motor (Fig. 6*C* and *D*) neurons. Figure 6*E*–*H* shows the response dynamic of neuronal populations with the same features recorded from area F5. For both areas, single-neuron and population activity is aligned to the visual presentation of the preferred target (left part of each panel) as well as to the onset of the reaching–grasping movement (right part). Several interesting differences emerge between the 2 areas. First, area F6 neurons are characterized by relatively shorter bursts of activity as compared with those of F5 (see Materials and Methods), and this finding is evident and consistent for both visuomotor (Fig. 6*A* and *E*) and purely motor (Fig. 6*B* and *G*) neurons considered separately (see also Supplementary Fig. S7*A* and *B*). Second, motor neurons of area F6 become active and peak earlier than those of area F5, where, in turn, most neurons display their activity peak in a restricted time window centered on the hand–object interaction (see Supplementary Fig. S7). Third, it is evident that many more neurons in F6 (Fig. 6*A* and *C*) than in F5 (Fig. 6*E* and *G*) alternate phases of increase and decrease in their activity: together with the above-mentioned features, this may explain the extremely different population response observed in the 2 areas (Fig. 6*B*, *D*, *F*, and *H*). Indeed, the neuronal population of F6 visuomotor neurons is characterized by a vigorous activation during the visual presentation of the target, at which point it also exhibits remarkable object selectivity, but it does not display any subsequent motor-related activation peak (Fig. 6*B*). In contrast, visuomotor neurons of area F5 display the typical visual-to-motor activation and selectivity pattern highlighted by several previous studies (Murata et al. 1997; Raos et al. 2006; Bonini et al. 2014a; Schaffelhofer et al. 2015), in which the motor-related discharge is even stronger than the visual one (Fig. 6*F*).

Further important differences emerged in terms of overall object selectivity. We showed that in area F6 there is a prevalence of visual selectivity for the ring (Fig. 4*C* and Supplementary Fig. S5) and no significant motor bias for any of the three tested objects (Fig. 3*C* and Supplementary Fig. S3). This finding is also evidenced in Figure 7*A*: a visual bias for the ring is exhibited by F6 visuomotor neurons from the visual presentation of the object until movement onset, whereas no significant bias emerged among purely motor neurons (Fig. 7*B*). In contrast, in area F5 we observed that both visuomotor (Fig. 7*C*) and purely motor (Fig. 7*D*) neurons displayed a strong motor bias in favor of the small cone (i.e., precision grip),

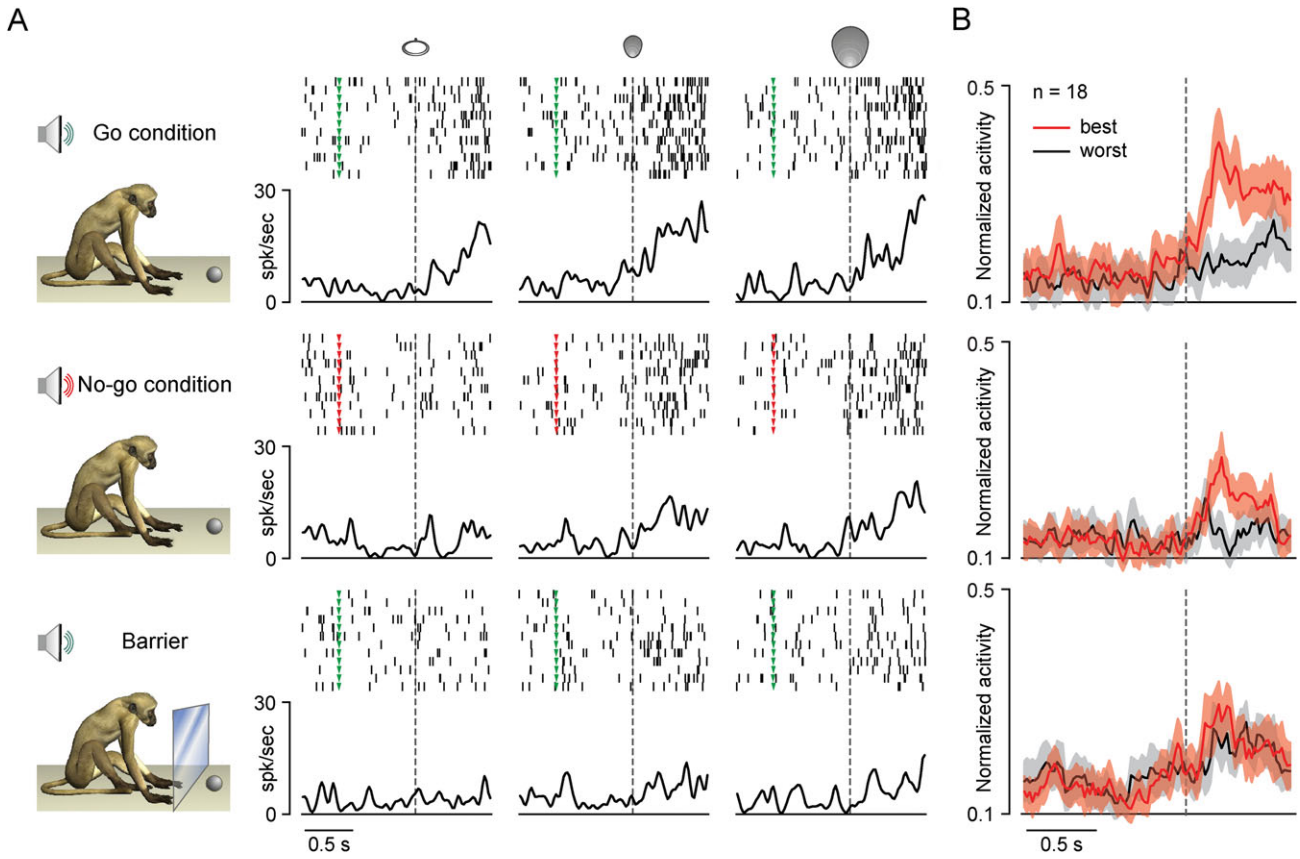

Figure 5. Visual responses of F6 neurons to object presentation in different contexts. (*A*) Example of an F6 visually-triggered neuron showing visual selectivity for the small and the big cone and reduced response and selectivity when tested with a plastic barrier interposed between monkey's hand and the target. Conventions as in Figure 1. (*B*) Population activity of all F6 visually-triggered neurons tested in the three conditions. The population responses to object presentation have been analyzed separately by means of 2 × 2 repeated measures ANOVAs (factors: Object and Epoch). The visual presentation response was stronger for the best relative to the worst object during both go and no-go conditions ($P < 0.001$ for both post hoc comparisons), but not during the barrier test ($P = 0.32$). Furthermore, the population response to the presentation of the best object was stronger when it occurred during go relative to no-go trials ($t = 3.09$, $P < 0.001$), while it was not different between no-go trials and those during the barrier test ($t = 0.015$, $P = 0.99$). The population response to the presentation of the worst object did not differ significantly among any of the compared conditions (go vs. no-go trials: $t = 0.82$, $P = 0.42$; go vs. barrier: $t = -1.09$, $P = 0.29$; no-go vs. barrier: $t = -1.99$, $P = 0.063$).

including a preparatory component that is more evident in purely motor neurons. Altogether, these findings suggest that whereas in F6 there is a prevalence of visuo-preparatory selectivity for the ring, which was subject to the more intensive visuomotor training, in F5 prevails the motor representation of the precision grip, which is one of the most natural and widespread types of grip (Macfarlane and Graziano 2009) typically used by monkeys to grasp and manipulate objects with no need of any explicit training.

Discussion

According to several neurophysiological studies, the pre-supplementary motor cortex plays a crucial role in complex sequential and cognitive processes underlying simple movements required as a response in a behavioral task (Tanji 2001; Akkal et al. 2004; Shima and Tanji 2006; Nakajima et al. 2009; Lucchetti et al. 2012). Another view maintains that the pre-supplementary motor cortex is involved in the specification of "whether" and "when" to perform an intended action (Haggard 2008), particularly in complex "cognitive" situations (Nachev et al. 2008). By contrast, encoding "what" an action should be and "how" it must be performed is thought to involve the parieto-frontal system (Rizzolatti et al. 2014).

Here we show for the first time that, in addition to a large set of neurons showing an uncommitted activation during vision and/or grasping of objects, in line with the well-established role of F6 in motor preparation, another set of F6 neurons also contribute to the visuomotor processing of objects and how they could be grasped. The same type of task of the present study has been typically used to investigate the properties of neurons in other areas of the cortical grasping network. Indeed, our findings indicate that a subset of F6 neurons can exhibit object-selective visual and motor responses. Most interestingly, visuomotor and purely motor F6 neurons appear to form 2 functionally distinct populations, in striking contrast to the dynamic visual-to-motor processing displayed by F5 visuomotor single-neuron and population activity. Furthermore, the visual processing of objects by area F6 neurons appears to be context-dependent, because neuronal selectivity was stronger when target presentation occurred in the context of go trials relative to no-go trials, and was completely abolished when, in spite of the instruction to go, a transparent barrier was interposed between the monkey's hand and the target, preventing the animal from reaching it. Altogether, these findings suggest that F6 visual activity can provide a motor representation of the impending object-directed action, which is conditional upon both the monkey's intention and possibility to perform it.

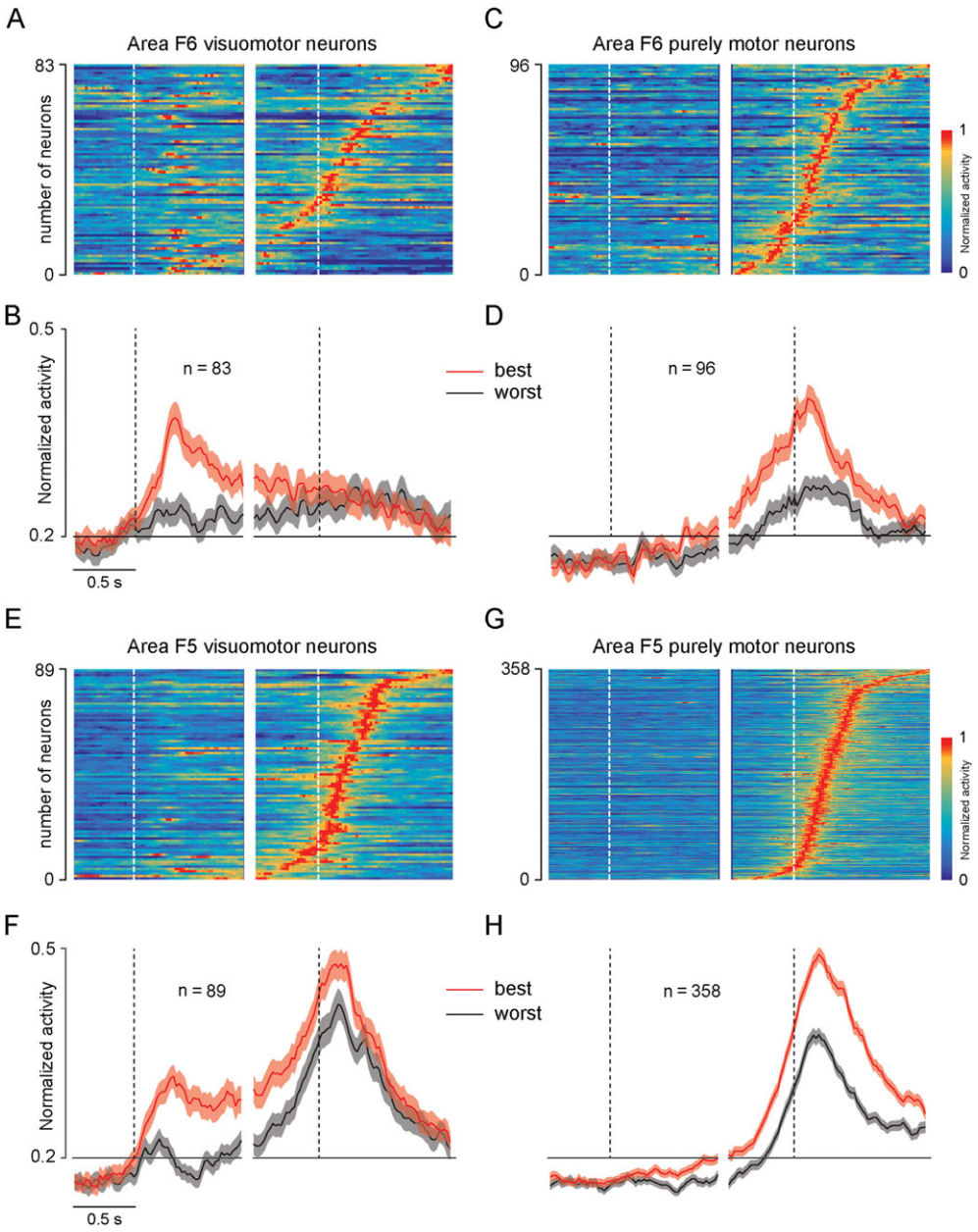

Figure 6. Comparison of neuronal dynamic and object selectivity between F5 and F6 visuomotor and purely motor neurons. Normalized activity of (*A*) visuomotor and (*C*) purely motor neurons of area F6 ordered based on the timing of their peak of motor activity (earliest on bottom). Each row represents a single neuron. White dashed lines represent the different alignment events: first (on the left, before the gap) object presentation, second (on the right, after the gap) hand movement onset. (*B* and *D*) Averaged population activity of the visuomotor (*B*) and purely motor (*D*) neurons of area F6 shown in (*A*) and (*C*). Black dashed lines correspond to the same alignment events described in (*A*) and (*C*). Other conventions as in Figure 4*B*. (*E*–*H*) Normalized single neuron (*E* and *G*) and population (*F* and *H*) activity of visuomotor and purely motor neurons recorded from area F5 of the same animals and with the same task. All conventions as in (*A*–*D*).

Anatomo-Functional Evidence of a Role of F6 in the Grasping Network

One of the most striking findings in the anatomical literature concerning area F6 is that, as compared with the adjacent supplementary motor area F3, it completely lacks direct connections with the spinal cord and the primary motor cortex (He et al. 1993; Luppino et al. 1993), in line with its low electrical excitability demonstrated by both the present and previous (Luppino et al. 1991) studies. Hence, its contribution to grasping actions has to be mediated by other anatomically connected areas.

Anatomical connections with area F6 have in fact been demonstrated for all the main premotor (Matelli et al. 1986; Luppino et al. 2003; Gerbella et al. 2011) as well as parietal (Luppino et al. 1993; Lewis and Van Essen 2000; Rozzi et al. 2006; Gamberini et al. 2009) nodes of the grasping network. Furthermore, F6 is consistently linked with the prefrontal cortex, particularly with the intermediate part of the convexity and bank portions of both dorsal (Saleem et al. 2014) and ventral (Gerbella et al. 2013) area 46. Interestingly, in this latter sector, neurons related to reaching–grasping actions have been recently described (Simone et al. 2015), and have been shown to exhibit visuomotor properties and context-dependent

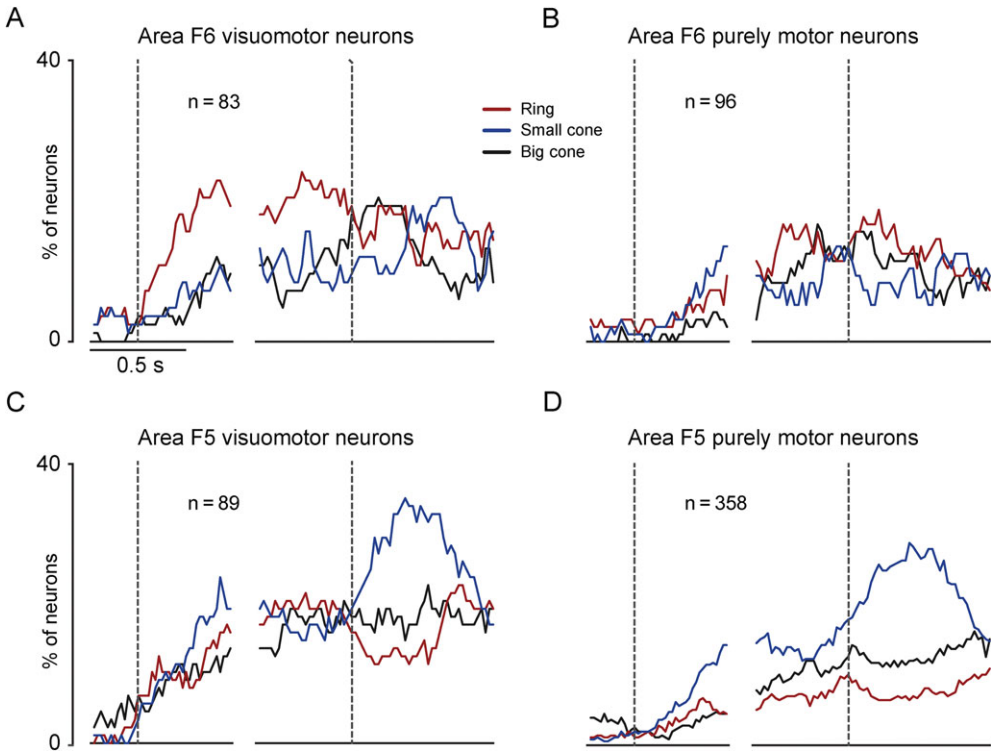

Figure 7. Comparison of object visual and motor selectivity of F5 and F6 neurons. (*A–D*) Each plot shows the percentage of neurons of each category and in each area exhibiting selectivity for one of the three tested objects during go-trials in the light (sliding 1-way repeated measures ANOVA, factor: Object, $P < 0.05$ uncorrected: see Materials and Methods).

modulations (Bruni et al. 2015). Finally, area F6 is also heavily connected with sectors of the basal ganglia (Parthasarathy et al. 1992; Takada et al. 2001) where neurons with hand-related motor responses have been described (Crutcher and DeLong 1984; Alexander and DeLong 1985). In summary, anatomical data support the possibility that F6 plays a role in reaching–grasping actions by integrating a wide range of information and influencing, both directly and indirectly, the processing operations carried out by the core areas of the grasping network.

The findings of the present study provide direct functional evidence in favor of this view by demonstrating that almost 26% of F6 task-related neurons display object/grip selectivity. Although this percentage is clearly lower than that obtained for area F5 (41%), there are several additional similarities between object processing in the 2 areas, strengthening the idea of their functional interplay. First, we showed that neuronal discharge and object selectivity of F6 purely motor neurons were the same during grasping in both the light and the dark, indicating that their activity truly reflects a motor encoding of the hand grip, as previously shown for F5 (Raos et al. 2006; Schaffelhofer et al. 2015). Second, both the visual presentation response and object selectivity of F6 visuomotor neurons were stronger during go trials, which is consistent with previous findings in F5 (Raos et al. 2006; Bonini et al. 2014a), and suggests that visuomotor neurons of both areas encode visually presented objects in a motor format. Third, the barrier test revealed that object selectivity was abolished when a transparent barrier was interposed between the monkey's hand and the target, as demonstrated for area F5 visuomotor neurons (see Bonini et al. 2014a), indicating that both areas underlie a "pragmatic description" of observed objects.

In spite of the functional analogies so far described and the tight reciprocal anatomical connections between F6 and F5 that could account for them, it is unlikely that these 2 areas provide a similar contribution to grasping actions. For example, it has been directly demonstrated that the inactivation of area F5 in monkeys impairs visually guided grasping of objects, providing causal evidence that this region plays a crucial role in controlling the hand shape for appropriately interacting with the target (Fogassi et al. 2001). In contrast, reaching–grasping actions are virtually unimpaired following large lesions of the pre-supplementary motor cortex (Brinkman and Porter 1983; Thaler et al. 1995). These findings would suggest that normal manual behavior is the result of a control exerted by mesial premotor areas on the lateral premotor cortex. Our data reveal that area F6 can play a role in the visuomotor representation of objects and of how they can be grasped, and provide the opportunity for a direct comparison with the functional properties of area F5 neurons.

The Relative Contribution of F6 and F5 to Reaching–Grasping Actions: Visuomotor Associations and Transformations

Convergent evidence from several studies indicates the existence of a typical visual-to-motor response pattern in all the parietal (Sakata et al. 1995; Rozzi et al. 2008; Baumann et al. 2009; Fattori et al. 2012; Fattori et al. 2015) and premotor (Murata et al. 1997; Raos et al. 2006; Fluet et al. 2010; Bonini et al. 2014a; Vargas-Irwin et al. 2015) nodes of the grasping network, particularly in F5 (see also Fig. 6*F*). This property has been classically deemed to reflect the visuomotor transformation of objects' physical properties into the motor acts most appropriate for interacting with them (Jeannerod et al. 1995).

Based on the fundamental differences we found between the single neuron and population activity of F6 and F5, it appears to be unlikely that F6 neurons play a role in visuomotor transformation. Instead, an interesting and more plausible interpretation can be suggested by considering the specific aspects of the neuronal visuomotor processing that characterize the 2 areas.

Our findings show that area F6 single neurons peak relatively earlier and display shorter bursts of phasic activity relative to those of F5 (Fig. 6), which, in contrast, exhibit a more sustained activity tuned on the hand–object interaction. At the population level, these differences translate into even more clear-cut evidence: though being anatomically intermingled, like those of F5 (Bonini et al. 2014a), visuomotor and purely motor F6 neurons form 2 functionally distinct populations. The former provides mainly a visual processing of the object (Fig. 6B and 7A), whereas the latter underlies a motor encoding of the grip type (Fig. 6C and 7B). In line with this difference, we also found a set of F6 neurons with purely visual response properties (see Table 1), which are virtually absent in area F5. Interestingly, area F6 purely visual neurons can also display contextual selectivity for go or no-go trials (see the example Neuron 1 in Fig. 6A), confirming the general role of F6 visually-triggered neurons in motor-related functions. More importantly, we observed a clear difference in the tuning for specific objects between the 2 areas. Indeed, F6 exhibited a bias in its visual and preparatory activity for the ring (i.e., hook grip), whereas F5 displayed a strong motor bias in favor of the small cone (i.e., precision grip). This finding suggests that in F6 the processing of overlearned visuomotor associations prevails, whereas in F5 there is a preferential coding of the visuomotor transformations related to the grip types belonging to the monkey's natural behavioral repertoire (Macfarlane and Graziano 2009).

How could visuomotor transformation and association processes interact? Typically, the same object can offer multiple grip affordances. Among them, we select the most appropriate depending on the current contextual situation, the goal we are pursuing, or specific instructions. Interestingly, Fluet et al. (2010) showed that ventral premotor neuronal representations of specific grip types (i.e., precision or power grip) to be employed for grasping the same handle can be triggered by the presentation of abstract visual cues (white or green spots of light) previously associated with the instructed grip type. Furthermore, using a similar paradigm, Vargas-Irwin et al. (2015) revealed that premotor neurons can dynamically integrate information related to the visual features of an observed object with the subsequently presented instructional cues for how to grasp it. Therefore, it is clear that in area F5, the visuomotor transformation of an object's visual features into the motor plans required for grasping it are flexibly modulated by learned visuomotor associations. The present findings suggest that F6 may encode visuomotor associations between specific elements of contextual information, likely conveyed by the prefrontal cortex, and motor representations of reaching–grasping actions. Although a similar role might be hypothesized for other ventral frontal regions connected with F6, such as the so-called pre-PMv (Dancause et al. 2008) or area F5a (Gerbella et al. 2011) and granular opercular frontal area (Gerbella et al. 2016), the present findings suggest that F6 could contribute to add contextual flexibility to the visuomotor transformations of the cortical grasping network.

Conclusions

The present findings are in line with previous proposals (Rizzolatti and Luppino 2001) maintaining that area F6 constitutes a prefronto-dependent area that forms a bridge between highly cognitive, context-based neuronal operations, on one side, and the parieto-dependent visuomotor transformations underlying the flow of voluntary actions, on the other. However, our findings also suggest to extend the existing models of the organization of reaching–grasping intentional actions (Fagg and Arbib 1998) by including the pre-supplementary motor area as a relevant, additional node of the cortical grasping network that plays a role in the integration of visuomotor transformation and sensorimotor association processes for action organization

Supplementary Material

Supplementary material can be found at: http://www.cercor.oxfordjournals.org/.

Funding

Istituto Italiano di Tecnologia and the European Commission Grant Cogsystem (FP7-250013) and received partial funding by BrainLinks-BrainTools Cluster of Excellence funded by the German Research Foundation (DFG, grant number EXC 1086).

Notes

Conflict of Interest: None declared.

References

Akkal D, Escola L, Bioulac B, Burbaud P. 2004. Time predictability modulates pre-supplementary motor area neuronal activity. Neuroreport. 15(8):1283–1286.

Alexander GE, DeLong MR. 1985. Microstimulation of the primate neostriatum. II. Somatotopic organization of striatal microexcitable zones and their relation to neuronal response properties. J Neurophysiol. 53(6):1417–1430.

Barz F, Paul O, Ruther P. 2014. Modular assembly concept for 3D neural probe prototypes offering high freedom of design and alignment precision. Conf Proc IEEE Eng Med Biol Soc. 80(10):6944495.

Baumann MA, Fluet M-C, Scherberger H. 2009. Context-specific grasp movement representation in the macaque anterior intraparietal area. J Neurosci. 29(20):6436–6448.

Belmalih A, Borra E, Contini M, Gerbella M, Rozzi S, Luppino G. 2007. A multiarchitectonic approach for the definition of functionally distinct areas and domains in the monkey frontal lobe. J Anat. 211(2):199–211.

Bettio F, Demelio S, Gobbetti E, Luppino G, Matelli M. 2001. Interactive 3-D reconstruction and visualization of primates cerebral cortex. Soc Neurosci Abstr p. 728:724.

Bonini L, Rozzi S, Serventi FU, Simone L, Ferrari PF, Fogassi L. 2010. Ventral premotor and inferior parietal cortices make distinct contribution to action organization and intention understanding. Cereb Cortex. 20(6):1372–1385.

Bonini L, Maranesi M, Livi A, Bruni S, Fogassi L, Holzhammer T, Paul O, Ruther P. 2014. Application of floating silicon-based linear multielectrode arrays for acute recording of single neuron activity in awake behaving monkeys. Biomed Tech. 59(4):273–281.

Bonini L, Maranesi M, Livi A, Fogassi L, Rizzolatti G. 2014a. Space-dependent representation of objects and other's action in monkey ventral premotor grasping neurons. J Neurosci. 34(11):4108–4119.

Bonini L, Maranesi M, Livi A, Fogassi L, Rizzolatti G. 2014b. Ventral premotor neurons encoding representations of action during self and others' inaction. Curr Biol. 24(14): 1611–1614.

Brinkman C, Porter R. 1983. Supplementary motor area and premotor area of monkey cerebral cortex: functional organization and activities of single neurons during performance of a learned movement. Adv Neurol. 39:393–420.

Bruni S, Giorgetti V, Bonini L, Fogassi L. 2015. Processing and integration of contextual information in monkey ventrolateral prefrontal neurons during selection and execution of goal-directed manipulative actions. J Neurosci. 35(34): 11877–11890.

Bruni S, Giorgetti V, Fogassi L, Bonini L. 2015. Multimodal encoding of goal-directed actions in monkey ventral premotor grasping neurons. Cereb Cortex. 22.

Cisek P, Kalaska JF. 2010. Neural mechanisms for interacting with a world full of action choices. Annu Rev Neurosci. 33: 269–298.

Crutcher MD, DeLong MR. 1984. Single cell studies of the primate putamen. I. Functional organization. Exp Brain Res. 53 (2):233–243.

Dancause N, Duric V, Barbay S, Frost SB, Stylianou A, Nudo RJ. 2008. An additional motor-related field in the lateral frontal cortex of squirrel monkeys. Cerebral Cortex. 18:2719–2728.

Davare M, Kraskov A, Rothwell JC, Lemon RN. 2011. Interactions between areas of the cortical grasping network. Curr Opin Neurobiol. 21(4):565–570.

Fagg AH, Arbib MA. 1998. Modeling parietal–premotor interactions in primate control of grasping. Neural Netw. 11(7): 1277–1303.

Fattori P, Raos V, Breveglieri R, Bosco A, Marzocchi N, Galletti C. 2010. The dorsomedial pathway is not just for reaching: grasping neurons in the medial parieto-occipital cortex of the macaque monkey. J Neurosci. 30(1):342–349.

Fattori P, Breveglieri R, Raos V, Bosco A, Galletti C. 2012. Vision for action in the macaque medial posterior parietal cortex. J Neurosci. 32(9):3221–3234.

Fattori P, Breveglieri R, Bosco A, Gamberini M, Galletti C. 2015. Vision for prehension in the medial parietal cortex. Cereb Cortex. doi:10.1093/cercor/bhv302.

Fluet M-C, Baumann MA, Scherberger H. 2010. Context-specific grasp movement representation in macaque ventral premotor cortex. J Neurosci. 30(45):15175–15184.

Fogassi L, Gallese V, Buccino G, Craighero L, Fadiga L, Rizzolatti G. 2001. Cortical mechanism for the visual guidance of hand grasping movements in the monkey: a reversible inactivation study. Brain. 124:571–586.

Gamberini M, Passarelli L, Fattori P, Zucchelli M, Bakola S, Luppino G, Galletti C. 2009. Cortical connections of the visuomotor parietooccipital area V6Ad of the macaque monkey. J Comp Neurol. 513(6):622–642.

Gerbella M, Belmalih A, Borra E, Rozzi S, Luppino G. 2011. Cortical connections of the anterior (F5a) subdivision of the macaque ventral premotor area F5. Brain Struct Funct. 216 (1):43–65.

Gerbella M, Borra E, Tonelli S, Rozzi S, Luppino G. 2013. Connectional heterogeneity of the ventral part of the macaque area 46. Cereb Cortex. 23(4):967–987.

Gerbella M, Borra E, Rozzi S, Luppino G. 2016. Connections of the macaque Granular Frontal Opercular (GrFO) area: a possible neural substrate for the contribution of limbic inputs for controlling hand and face/mouth actions. Brain Struct Funct. 221(1):59–78.

Grafton ST. 2010. The cognitive neuroscience of prehension: recent developments. Exp Brain Res. 204(4):475–491.

Haggard P. 2008. Human volition: towards a neuroscience of will. Nat Rev Neurosci. 9(12):934–946.

He SQ, Dum RP, Strick PL. 1993. Topographic organization of corticospinal projections from the frontal lobe: motor areas on the lateral surface of the hemisphere. J Neurosci. 13(3): 952–980.

Herwik S, Paul O, Ruther P. 2011. Ultrathin silicon chips of arbitrary shape by etching before grinding. J Microelectromech Syst. 20(4):791–793.

Jeannerod M, Arbib MA, Rizzolatti G, Sakata H. 1995. Grasping objects: the cortical mechanisms of visuomotor transformation. Trends Neurosci. 18(7):314–320.

Kaas JH, Stepniewska I. 2016. Evolution of posterior parietal cortex and parietal-frontal networks for specific actions in primates. J Comp Neurol. 524(3):595–608.

Lewis JW, Van Essen DC. 2000. Corticocortical connections of visual, sensorimotor, and multimodal processing areas in the parietal lobe of the macaque monkey. J Comp Neurol. 428(1):112–137.

Lucchetti C, Lanzilotto M, Perciavalle V, Bon L. 2012. Neuronal activity reflecting progression of trials in the presupplementary motor area of macaque monkey: an expression of neuronal flexibility. Neurosci Lett. 506(1):33–38.

Luppino G, Matelli M, Camarda R, Gallese V, Rizzolatti G. 1991. Multiple representations of body movements in mesial area 6 and the adjacent cingulate cortex: an intracortical microstimulation study in the macaque monkey. J Comp Neurol. 311(4):463–482.

Luppino G, Matelli M, Camarda R, Rizzolatti G. 1993. Corticocortical connections of area F3 (SMA-proper) and area F6 (pre-SMA) in the macaque monkey. J Comp Neurol. 338(1):114–140.

Luppino G, Rozzi S, Calzavara R, Matelli M. 2003. Prefrontal and agranular cingulate projections to the dorsal premotor areas F2 and F7 in the macaque monkey. Eur J Neurosci. 17(3):559–578.

Macfarlane NB, Graziano MS. 2009. Diversity of grip in Macaca mulatta. Exp Brain Res. 197(3):255–268.

Maranesi M, Bonini L, Fogassi L. 2014. Cortical processing of object affordances for self and others' action. Front Psychol. 5:538.

Maranesi M, Livi A, Bonini L. 2015. Processing of own hand visual feedback during object grasping in ventral premotor mirror neurons. J Neurosci. 35(34):11824–11829.

Matelli M, Camarda R, Glickstein M, Rizzolatti G. 1986. Afferent and efferent projections of the inferior area 6 in the macaque monkey. J Comp Neurol. 251(3):281–298.

Matelli M, Luppino G, Rizzolatti G. 1991. Architecture of superior and mesial area 6 and the adjacent cingulate cortex in the macaque monkey. J Comp Neurol. 311(4):445–462.

Murata A, Fadiga L, Fogassi L, Gallese V, Raos V, Rizzolatti G. 1997. Object representation in the ventral premotor cortex (area F5) of the monkey. J Neurophysiol. 78(4):2226–2230.

Nachev P, Kennard C, Husain M. 2008. Functional role of the supplementary and pre-supplementary motor areas. Nat Rev Neurosci. 9(11):856–869.

Nakajima T, Hosaka R, Mushiake H, Tanji J. 2009. Covert representation of second-next movement in the presupplementary motor area of monkeys. J Neurophysiol. 101 (4):1883–1889.

Nakamura K, Sakai K, Hikosaka O. 1998. Neuronal activity in medial frontal cortex during learning of sequential procedures. J Neurophysiol. 80(5):2671–2687.

Parthasarathy HB, Schall JD, Graybiel AM. 1992. Distributed but convergent ordering of corticostriatal projections: analysis of the frontal eye field and the supplementary eye field in the macaque monkey. J Neurosci. 12(11):4468–4488.

Raos V, Umiltá MA, Gallese V, Fogassi L. 2004. Functional properties of grasping-related neurons in the dorsal premotor area F2 of the macaque monkey. J Neurophysiol. 92(4): 1990–2002.

Raos V, Umiltá MA, Murata A, Fogassi L, Gallese V. 2006. Functional properties of grasping-related neurons in the ventral premotor area F5 of the macaque monkey. J Neurophysiol. 95(2):709–729.

Rizzolatti G, Gentilucci M, Camarda R, Gallese V, Luppino G, Matelli M, Fogassi L. 1990. Neurons related to reaching-grasping arm movements in the rostral part of area 6 (area 6aβ). Exp Brain Res. 82(2):337–350.

Rizzolatti G, Luppino G. 2001. The cortical motor system. Neuron. 31(6):889–901.

Rizzolatti G, Cattaneo L, Fabbri-Destro M, Rozzi S. 2014. Cortical mechanisms underlying the organization of goal-directed actions and mirror neuron-based action understanding. Physiol Rev. 94(2):655–706.

Rozzi S, Calzavara R, Belmalih A, Borra E, Gregoriou GG, Matelli M, Luppino G. 2006. Cortical connections of the inferior parietal cortical convexity of the macaque monkey. Cereb Cortex. 16(10):1389–1417.

Rozzi S, Ferrari PF, Bonini L, Rizzolatti G, Fogassi L. 2008. Functional organization of inferior parietal lobule convexity in the macaque monkey: electrophysiological characterization of motor, sensory and mirror responses and their correlation with cytoarchitectonic areas. Eur J Neurosci. 28(8): 1569–1588.

Sakata H, Taira M, Murata A, Mine S. 1995. Neural mechanisms of visual guidance of hand action in the parietal cortex of the monkey. Cereb Cortex. 5(5):429–438.

Saleem KS, Miller B, Price JL. 2014. Subdivisions and connectional networks of the lateral prefrontal cortex in the macaque monkey. J Comp Neurol. 522(7):1641–1690.

Schaffelhofer S, Agudelo-Toro A, Scherberger H. 2015. Decoding a wide range of hand configurations from macaque motor, premotor, and parietal cortices. J Neurosci. 35(3):1068–1081.

Shima K, Tanji J. 2006. Binary-coded monitoring of a behavioral sequence by cells in the pre-supplementary motor area. J Neurosci. 26(9):2579–2582.

Simone L, Rozzi S, Bimbi M, Fogassi L. 2015. Movement-related activity during goal-directed hand actions in the monkey ventrolateral prefrontal cortex. Eur J Neurosci. 42(11): 2882–2894.

Takada M, Tokuno H, Hamada I, Inase M, Ito Y, Imanishi M, Hasegawa N, Akazawa T, Hatanaka N, Nambu A. 2001. Organization of inputs from cingulate motor areas to basal ganglia in macaque monkey. Eur J Neurosci. 14(10): 1633–1650.

Tanji J. 2001. Sequential organization of multiple movements: involvement of cortical motor areas. Annu Rev Neurosci. 24: 631–651.

Thaler D, Chen YC, Nixon PD, Stern CE, Passingham RE. 1995. The functions of the medial premotor cortex. I. Simple learned movements. Exp Brain Res. 102(3):445–460.

Vargas-Irwin CE, Franquemont L, Black MJ, Donoghue JP. 2015. Linking objects to actions: encoding of target object and grasping strategy in primate ventral premotor cortex. J Neurosci. 35(30):10888–10897.